NOTICE

AVIS

The quality of this microform is heavily dependent upon the quality of the original thesis submitted for microfilming. Every effort has been made to ensure the highest quality of reproduction possible.

If pages are missing, contact the university which granted the degree.

Some pages may have indistinct print especially if the original pages were typed with a poor typewriter ribbon or if the university sent us an inferior photocopy.

Previously copyrighted materials (journal articles, published tests, etc.) are not filmed.

Reproduction in full or in part of this microform is governed by the Canadian Copyright Act, R.S.C. 1970, c. C-30.

La qualité de cette microforme dépend grandement de la qualité de la thèse soumise au microfilmage. Nous avons tout fait pour assurer une qualité supérieure de reproduction.

S'il manque des pages, veuillez communiquer avec l'université qui a conféré le grade.

La qualité d'impression de certaines pages peut laisser à désirer, surtout si les pages originales ont été dactylographiées à l'aide d'un ruban usé ou si l'université nous a fait parvenir une photocopie de qualité inférieure.

Les documents qui font déjà l'objet d'un droit d'auteur (articles de revue, tests publiés, etc.) ne sont pas microfilmés.

La reproduction, même partielle, de cette microforme est soumise à la Loi canadienne sur le droit d'auteur, SRC 1970, c. C-30.

Canada

THE UNIVERSITY OF ALBERTA

ULTRASONIC ATTENUATION IN CeAl$_2$ BELOW 4K.

by

William A. Miner

A THESIS

SUBMITTED TO THE FACULTY OF GRADUATE STUDIES AND RESEARCH

IN PARTIAL FULFILMENT OF THE REQUIREMENTS FOR THE DEGREE

OF MASTER OF SCIENCE

IN

LOW TEMPERATURE PHYSICS

DEPARTMENT OF PHYSICS

EDMONTON, ALBERTA

SPRING 1988

THE UNIVERSITY OF ALBERTA

RELEASE FORM

NAME OF AUTHOR: William A. Miner.

TITLE OF THESIS: ULTRASONIC ATTENUATION IN $CeAl_2$ BELOW 4K.

DEGREE FOR WHICH THESIS WAS PRESENTED: MASTER OF SCIENCE

YEAR THIS DEGREE GRANTED: SPRING 1988

Permission is hereby granted to THE UNIVERSITY OF ALBERTA LIBRARY to reproduce single copies of this thesis and to lend or sell such copies for private, scholarly or scientific research purposes only.

The author reserves other publication rights, and neither the thesis nor extensive extracts from it may be printed or otherwise reproduced without the author's written permission.

(SIGNED) *Bill. A. Miner*

PERMANENT ADDRESS:

Box 194,

Mayerthorpe, Alberta

T0E 1N0

DATED 22 April 1988

THE UNIVERSITY OF ALBERTA

FACULTY OF GRADUATE STUDIES AND RESEARCH

The undersigned certify that they have read,
and recommend to the Faculty of Graduate Studies and
Research for acceptance, a thesis entitled ULTRASONIC
ATTENUATION IN $CeAL_2$ BELOW 4K submitted by William A.
Miner in partial fulfilment of the requirements for the
degree of MASTER OF SCIENCE in PHYSICS.

....

Supervisor

....

....

....

Date ..21. April..1988..

DEDICATION

To my parents, for their support and encouragement.

ABSTRACT

$CeAl_2$ is a rare earth intermetallic compound that has been classified as a dense Kondo material, although it is also closely related to the so called heavy fermion systems. $CeAl_2$ displays complex antiferromagnetic order below 3.9K. This is unusual behaviour as the presence of the Kondo effect usually precludes coherent behaviour. There is some question about the exact nature of the H-T phase diagram of $CeAl_2$ near the phase transition. It is possible that a second magnetic transition exists, very close to the known transition at 3.9K, as there is in the closely related compound, CeB_6.

Ultrasonic attenuation is very sensitive to magnetic phase transitions and thus makes an excellent tool with which to examine the H-T phase diagram of $CeAl_2$.

This work describes ultrasonic attenuation measurements made on a polycrystalline sample of $CeAl_2$ in an attempt to elucidate this magnetic phase structure.

ACKNOWLEDGEMENT

Table of Contents

LIST OF FIGURES

1. INTRODUCTION

The rare-earth intermetallic compound $CeAl_2$ has several unusual properties and, as a result, has been the subject of considerable study in recent years. In addition to being a dense Kondo material with complex order at low temperatures, $CeAl_2$ is also related to the so-called heavy fermion or heavy electron systems.

Heavy electron systems have been under intensive investigation recently because of their unusually high electronic specific heat coefficients, γ, and their anomalous low temperature ordering behaviour [Stewart, 1984].

At low temperatures the specific heat in a normal metal is described by:

$$(1-1) \qquad C = \gamma T + \beta T^3$$

where γ is called the electronic specific heat coefficient, and β is the phonon or lattice specific heat coefficient. With this sort of behaviour a graph of C/T vs. T^2 gives a straight line with γ being the intercept on the C/T axis.

For a normal metal, γ is typically about 1 $mJ/K^2 mole$. However, in heavy electron systems the electronic specific heat coefficient at low temperatures is as much as three orders of magnitude larger. Such a large γ implies either a very large electron density of states, or a large electron effective mass.

The electronic specific heat coefficient of $CeAl_2$ is about 135 mJ/K^2mole [Bredl et al. 1978; Armbruster & Steglich, 1978]. Though not as high as the typical heavy electron materials, this value of γ for $CeAl_2$ is clearly very much larger than that for an ordinary metal.

This, and other evidence [Patthey et al. 1987] suggests not only that $CeAl_2$ is closely related to the heavy electron systems, but that $CeAl_2$ would actually be classed as a heavy electron system were it not for the magnetic ordering that takes place below 4K.

The circumstances surrounding the magnetic ordering of $CeAl_2$ have generated a lot of interest in this compound. It was only in 1977 that the nature of the phase transition at 3.9K was determined [Barbara et al. 1977], and even now there are some indications of a second phase transition in the same vicinity [Schefzyk et al. 1985; Kadowaki, 1985], which would seem to indicate behaviour similar to that observed in CeB_6 [Rossat-Mignod et al. 1981].

This low temperature magnetic ordering in a dense Kondo material is another one of the unusual properties of $CeAl_2$. These are competing effects since both are due to the exchange interaction between the conduction electrons and the localized 4f electrons. Usually the presence of the Kondo effect precludes such magnetic ordering.

While it is very difficult to measure the ultrasonic attenuation at low temperatures, this technique was chosen

to explore the nature of the phase transition in $CeAl_2$ for several reasons. Ultrasonic attenuation is known to be a very sensitive tool for detecting phase transitions, therefore such measurements may be able to detect a second transition should it exist.

In addition to the techniques sensitivity to phase transitions, there is no mention in the literature of ultrasonic attenuation measurements being made on $CeAl_2$, although some very preliminary work by Kadowaki [1985] holds some promise.

2. THE KONDO EFFECT

2.1 Dilute Kondo Effect

The resistivity of ordinary metals is due to electron scattering by lattice vibrations, or phonons, and shows a monotonic decline with decreasing temperature toward some constant value. This residual resistivity is due to the scattering of electrons by non-magnetic impurities and lattice defects in the metal.

If, however, very small amounts of a magnetic impurity are dissolved in a non-magnetic metal, the localized moments of these ions act as scattering centres. At low temperatures these moments may become the most important contribution to the electrical resistivity.

The presence of these magnetic impurities significantly alters the low temperature behaviour of the resistivity. Instead of decreasing toward some residual value, the resistivity actually begins to increase with decreasing temperature and, combined with phonon scattering, produces a shallow resistance minimum [Ashcroft & Mermin, 1976].

This behaviour, while first noticed nearly sixty years ago [Meissner & Voigt, 1930], was first theoretically described by Kondo [1964], and hence is known as the Kondo effect.

Kondo showed that the resistance minimum was due to

previously unsuspected effects of the scattering of the conduction electrons by a magnetic impurity. Earlier analyses to leading order in perturbation theory had indicated that the magnetic and non-magnetic cases were qualitatively the same. Kondo showed, however, that to all higher orders the magnetic scattering cross-section is divergent as T goes to zero, implying an infinite resistivity. This divergence can be removed by considering the splitting of the localized spins [Kondo, 1964]. Since these splittings occur at temperatures much lower than those of interest, one can just use the straight forward result (which follows) remembering that the divergent term can be made convergent if required.

The result of Kondo's calculation is a spin-dependant contribution to the resistivity of:

$$(2-1) \qquad \rho = c\rho_M(1 + (3zJ/E_F)\ln T)$$

where J is the exchange energy, c is the impurity concentration, z the number of nearest neighbours, E_F is the Fermi energy, and ρ_M is a measure of the strength of the exchange scattering. Thus, if the exchange energy, J, is negative, the resistivity due to the magnetic scattering centres can be seen to increase with decreasing temperature. Writing the total resistivity as the sum (assuming that the individual parts can be added) of this Kondo spin scattering, the lattice resistivity ρ_L, and the resistivity caused by the impurity potential ρ_A, we have:

(2-2) $\quad \rho_{TOT} = \rho_L + c\rho_A + c\rho_M + c(3zJ\rho_M/E_F)\ln T$

If we assume that the lattice resistance goes as T^n ($n \lesssim 5$) and combine ρ_A and ρ_M into a new constant ρ_0, we can then write:

(2-3) $\quad \rho_{TOT} = aT^5 + c\rho_0 - c\rho_1\ln T$

with:

(2-4) $\quad \rho_1 = 3z|J|/E_F$

Differentiating with respect to T gives the location of the resistance minimum:

(2-5) $\quad d\rho_{TOT}/dT = 5aT^4 - c\rho_1/T = 0$

therefore:

(2-6) $\quad T_{min} = (c\rho_1/5a)^{1/5}$

2.2 Dense Kondo Effect

The above treatment considered only isolated magnetic impurities, and is therefore usually referred to as the "dilute" or single ion Kondo effect. Only very small amounts of the magnetic impurity are required to produce the resistance minimum. For example, 0.05% Fe dissolved in pure copper produces a very pronounced effect [Ashcroft & Mermin 1976, p687; Franck et al. 1961]. Moreover the resistance minimum is diminished as the impurity concentration is increased.

It is, therefore, quite surprising that one should

find, in certain rare earth compounds, a Kondo-like resistance minimum, since these are concentrated systems of local moments. That is, they are systems having a magnetic ion in every cell of the crystal [Doniach, 1977].

The single ion Kondo theory is inadequate in these circumstances and efforts are being made [Doniach, 1977; Ohkawa, 1983; Yoshimori & Kasai, 1984] to construct a theoretical framework for these compounds.

One of the features of these, so called, "dense Kondo" materials is that the f-level wave function is sufficiently localized on each magnetic ion that no direct f-f interaction can occur between neighbouring ions, and an indirect Kondo like effect occurs involving the conduction electrons on the other ions.

However, at low temperatures, some of these materials also exhibit coherent behaviour in spite of this apparent high degree of f-level localization [Ohkawa, 1983] i.e., these materials enter some sort of ordered state even though the magnetic sites seem to be completely independent at higher temperatures.

$CeAl_2$ and CeB_6 are such compounds. They order antiferromagnetically at sufficiently low temperatures.

3. $CeAl_2$

CeAl$_2$ is an interesting material in several respects. It is not only a magnetic lattice that displays Kondo behaviour (i.e. a dense Kondo material), but it also enters a complex ordered state at low temperatures. In addition, there is still some doubt as to the exact nature of the magnetic phase diagram.

$CeAl_2$ is a rare earth intermetallic compound that crystallizes in the cubic-Laves phase $MgCu_2$ structure [Walker et al. 1973]. The cerium atoms form a diamond type lattice, with four aluminum tetrahedra in each conventional unit cell as shown in figure 3-1. The tripositive [Croft et al. 1978] cerium ions thus experience a cubic crystalline electric field.

$CeAl_2$ has been characterized as a Kondo-type material by electrical resistivity measurements [Bredl et al. 1978; Onuki et al. 1984]. The resistivity curve clearly shows (figure 3-2) the characteristic shallow minimum that is created by the logarithmic change of the resistivity with temperature below the minimum. This curve has been fitted [Cornut & Coqblin, 1972] down to about 10K using a single impurity Kondo model that takes the crystal field effects into account. This model fails to produce the maximum observed in the resistivity (figure 3-2) at temperatures below the minimum.

This page has been removed because of the unavailability of copyright permission.

The page contained two figures: one showing the unit cell of $CeAl_2$ which was taken from a paper by Barbara et al. that appeared in Solid State Communications, 24, 1977, p481; and the other showing a typical resistivity curve for $CeAl_2$ taken from a paper by Bauer et al. that appeared in the Journal of Magnetism and Magnetic Materials, 29, 1982, p192.

A phase transition in $CeAl_2$ is indicated by anomalies in its resistivity [Buschow & van Daal, 1969], specific heat and magnetic susceptibility [Hill & da Silva, 1969; Bredl et al. 1978]. This transition occurs at about 3.9K, where neutron diffraction experiments show that the compound assumes a complex antiferromagnetic structure. Specifically the antiferromagnetic order consists of a sinusoidal spin density wave that is incommensurate with the crystal structure [Barbara et al. 1977].

The magnetic ordering is believed to be due to an indirect exchange mechanism that occurs between cerium ions in spite of the competing Kondo effect [Aarts et al. 1985]. The number of conduction electrons participating in the Kondo effect is insufficient to fully compensate, or weaken, the cerium ion magnetic moments. The opportunity for the appearance of such an ordered state might be provided only in those compounds where the Kondo and the competing interaction are suitably anisotropic.

Specific heat data [Bredl et al. 1978] seem to indicate that only about 10 per cent of the conduction band states are compensating the magnetic moments. Even so, the resulting Kondo effect is sufficient to suppress the transition temperature to 3.9K, whereas, if the indirect exchange mechanism was acting alone, the transition temperature might have been as high as 7K [Croft & Levine, 1980].

The possibility of a second magnetic transition in CeAl$_2$ is suggested by its similarity to the dense Kondo material CeB$_6$ [Rossat-Mignod et al. 1981]. In addition Schefzyk et al. [1985], have seen evidence of a second transition. Kadowaki [1985], in preliminary ultrasonic studies, has also noticed unusual behaviour which may be suggestive of a second magnetic transition.

If such a phase transition exists, it would have to be very close to the known transition, as the other transport properties do not show any extra anomalies. There would then be two T$_N$s, very close together in zero applied field, and becoming more distinct as the applied field is increased (figure 3-3).
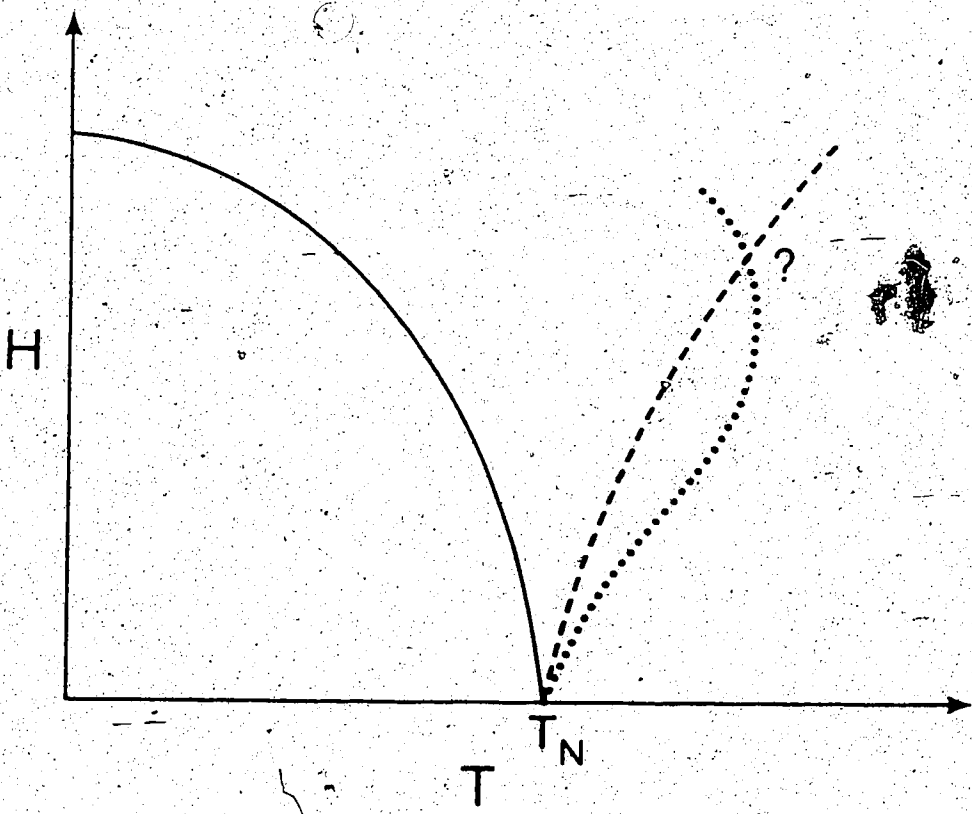
figure 3-3 Magnetic phase diagram showing
            possible unknown phase boundaries.

4. ULTRASONIC ATTENUATION

4.1 Introduction

The terms ultrasound or ultrasonic waves refer merely to sound waves that propagate at frequencies beyond the range of the human ear. Therefore mechanical vibrations having frequencies above about 16 kHz form part of the ultrasonic spectrum. The frequency range available to ultrasonic attenuation experiments using the pulse echo technique is limited by equipment concerns (e.g. electromagnetic losses) to between a few megahertz and a few hundred megahertz.

While these frequencies may seem to be high and the range fairly extensive, at least two orders of magnitude, they intersect only a very small part of the frequency spectrum of the thermal oscillations in a solid (see figure 4-1).

This overall spectrum is made up of mechanical vibrations that range from macroscopic regions moving against one another, at the lowest frequencies, to the oscillations of individual atoms, quantized as lattice waves, at the highest.

Even though the attainable ultrasonic frequencies represent such a small part of the lower end of this thermal spectrum, one can learn much about the transport mechanisms present by passing ultrasonic signals through the sample and observing how they are attenuated.

This page has been removed because of the unavailability of copyright permission.

The page contained a figure showing the phonon spectrum of a lattice at 1K. The figure was taken from a thesis by R. David that appeared in Philips Research Reports, 19, 1964, p524.

As the ultrasonic signal propagates through the specimen, energy is scattered out of the beam and/or absorbed by various means. In order to describe this energy loss an attenuation coefficient, α , having units of length^{-1}, is defined. An expression for α is usually obtained [Truell et al. 1969, p55] by considering a plane stress wave:

(4-1) $$\sigma(x,t) = \sigma_0 e^{i(\omega t - kx)}$$

where:

(4-2) $$k^2 v^2 = \omega^2$$

and writing an expression for the attenuated wave by assuming that the velocity, v, and the wave vector, k, are complex. With:

(4-3) $$v = v_1 + iv_2$$

(4-4) $$k = k_1 - i\alpha$$

the expression for $\sigma(x,t)$ becomes:

(4-5) $$\sigma(x,t) = \sigma_0 e^{-\alpha x} e^{i(\omega t - k_1 x)}$$

Because the ultrasonic attenuation is determined by the high frequency envelope, one can just use:

(4-6) $$\sigma(x) = \sigma_0 e^{-\alpha x}$$

as an expression from which the attenuation can be found.

Alternatively, the same result can be obtained [David, 1964] by considering the stress amplitude $|\sigma(x)|$ and how it decreases over a small distance dx. If the

decrease $d|\sigma(x)|$, is assumed to be proportional to the distance dx, the amplitude $|\sigma(x)|$ itself, and independent of the position x, one then has:

(4-7) $\quad\quad\quad d|\sigma(x)| = -\alpha|\sigma(x)|dx$

with the attenuation coefficient, α, entering the equation as the constant of proportionality. Integrating this expression, with σ_0 being the stress at zero distance gives:

(4-8) $\quad\quad\quad\quad |\sigma| = \sigma_0 e^{-\alpha x}$

which is the same as the previous result.

There are many mechanisms that contribute to the attenuation of an ultrasonic signal in a solid. For our purposes these mechanisms can be roughly placed into three categories:

a). <u>Non-dissipative attenuation</u>. This includes attenuation due to the scattering of the ultrasonic signal by impurities or imperfections in the crystal, or grain boundaries in polycrystalline materials. Other causes can include; lack of parallelism of the sample surfaces (which will be touched on later) and mode conversion (i.e. a longitudinal wave partially converted to transverse by anisotropic crystal properties, or by contact with the sides of a sample) [Beyer & Letcher, 1969, p242]. These

mechanisms are temperature independent and form a background peculiar to the specimen in question.

b). phonon-phonon interaction: The phonon wavetrain of the ultrasonic signal can interact with the thermal phonons present in the specimen in spite of the extremely large frequency difference between the two (recall figure 4-1). Ideally, if the waves were linearly elastic, there should be no interaction even between waves of equal frequency. However, this is not the case, as experiments show (see figure 4-2). One way that this interaction is thought to occur [Truell et al. 1969, p309] is that the passing sound waves disturb the equilibrium thermal phonon distribution. The thermal phonons seek to counter this disturbance via phonon processes not related to the sound beam and energy is removed from the system. For details of the calculation of the attenuation see Truell et al. [1969] and the references therein.

c). electron-phonon interaction: The curve in figure 4-2 showing the attenuation in Al_2O_3 is very typical of the attenuation in a

This page has been removed because of the unavailability of copyright permission.

The page contained a figure showing typical ultrasonic attenuation curves in an insulating material. The figure was taken from <u>Ultrasonic Methods in Solid State Physics</u> by Truell et al. 1969 Academic Press New York.

material with no free electrons present. The
attenuation decreases with temperature and
eventually reaches a constant value due to
impurity scattering. However, the case for a
metal is quite different. The attenuation is
found to increase again at temperatures below
about 20K. This low temperature increase in
attenuation with decreasing temperature is
attributed to the coupling between the
ultrasonic waves and the conduction electrons
[Bhatia, 1967, p290].

This electron-phonon coupling is thought to
arise [Pippard, 1955] from an internal
electric field set up when the lattice ions
are displaced by the passing of the
ultrasonic wave. The conduction electrons
are influenced by this field in addition to
the relaxation effects which try to re-
establish local equilibrium with the ordinary
mechanisms already present (thermal phonons,
impurities, etc.). This extra disruption
causes the electron distribution to be
different, at any given period, than the
distribution that would result if the
electrons were in local equilibrium with the

ions. This difference causes an irreversible loss of energy and the sound wave is attenuated. While Pippard's calculations using the above ideas were based on a semi-classical free electron model, a quantum mechanical approach [Morse, 1959] will give Pippard's result when the classical limit is taken [Truell et al. 1969, p293].

An alternative way to visualize the electron-phonon interaction is to consider the electron's mean free path [Mason, 1958, p319]. When the temperature is very low the electron mean free path becomes very large compared to its room temperature value, and begins to approach the phonon wavelength. When the electron mean free path becomes comparable to the phonon wavelength the electrons are then able to interact with the lattice vibrations and acquire momentum. This causes an irreversible loss of energy from the lattice waves, which appears as the ultrasonic attenuation.

In a normal metal these three scattering mechanisms

combine (figure 4-3) to form the overall, or total attenuation. If, however, the metal deviates from "normal" behaviour, e.g. undergoes a phase transition, one would expect the ultrasonic attenuation to change. The nature of this change in the attenuation will, of course, depend upon whether the change in the metal hinders or enhances the ability of the various scattering mechanisms to couple with the sound waves. In the superconducting phase transition, for example, the attenuation decreases rapidly (figure 4-3) as the conduction electrons "condense" into the Cooper-pair bound state, and are no longer able to scatter the sound wave [Bhatia, 1967, p317].

The change in the metal may even introduce another scattering source altogether. This is the case in magnetic transitions such as the one that occurs in $CeAl_2$. In such a transition between the paramagnetic and the antiferromagnetic states of an antiferromagnet, the ultrasonic attenuation peaks sharply near the Neel temperature. This peak is attributed [Luthi & Pollina, 1968; Ikushima, 1970] to a spin-phonon coupling mechanism which becomes important near the transition.

Although a spin-phonon interaction seems to be established as the cause of the attenuation anomaly, there has been considerable discussion about the exact nature of the interaction [Cracknell & Semmens, 1971; Itoh, 1975]. Most of these theories favour phonon scattering by critical
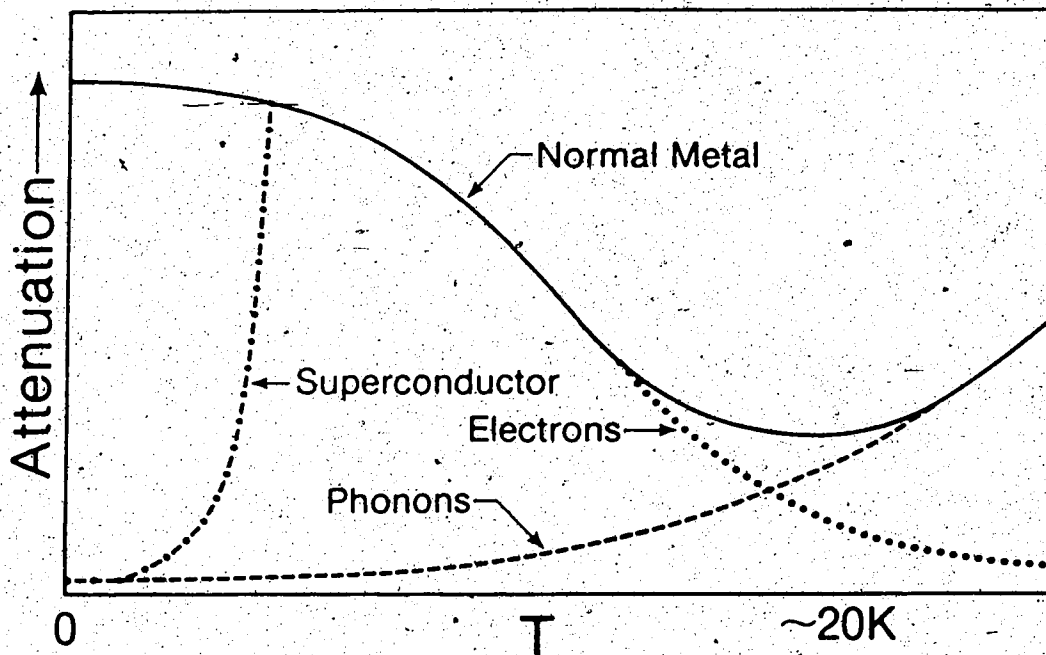
figure 4-3   Schematic diagram of ultrasonic
             attenuation in metals.
             [Bhatia, 1967, p291]

spin fluctuations, or some variation of the spin fluctuation idea [Luthi et al. 1970; Itoh, 1975; Ikushima, 1970] as being responsible for the attenuation of the sound wave. The phonons are thought to be scattered by fluctuations in the degree of spin order. These fluctuations become very large in the region of the ordering temperature, T_N, and as a result the sound waves have a large scattering cross section near T_N.

In order to derive the temperature and frequency dependence of the ultrasonic attenuation, all theories using the spin fluctuation approach begin with a very complicated expression for $\propto$ [Luthi et al. 1970]. This expression is derived from either the spin-phonon Hamiltonian, or an argument based on irreversible thermodynamics. This expression for $\propto$ is unworkable in its most complete form; therefore various assumptions and approximations are made to simplify $\propto$ and extract the required dependencies. Although different authors choose different methods [Luthi et al. 1970], and varying degrees of sophistication [Itoh, 1975], the results are, qualitatively, very similar. The expression for the attenuation is reduced to the form:

(4-9) $$\propto \propto \omega^2 x^1 / (1/\tau_c)$$

or:

(4-10) $$\propto \propto \omega^2 C_m / (1/\tau_c)$$

where X is the spin susceptibility, C_m is the magnetic
contribution to the specific heat, and τ_c is the
characteristic decay time of the critical spin fluctuations
(which is assumed to be much shorter than the phonon transit
time [Luthi et al. 1970]). The temperature dependence is
contained in the susceptibility (or the specific heat),
which show peaks [Wielinga, 1970] at the transition. These
peaks are enhanced by the $1/\tau_c$ term, as τ_c diverges near T_N.

The temperature dependence can also be written
explicitly [Luthi et al. 1970] as:

(4-11) $\qquad\qquad \propto \propto \omega^2 \, |(T-T_N)/T_N|^{-n}$

for temperatures close to the transition temperature, T_N. A
typical curve is that of the antiferromagnetic transition of
MnF_2 shown in figure 4-4.

The various theories are then tested by comparing
the theoretically and experimentally determined critical
exponents (n).

While these theories based on critical fluctuation
ideas are, qualitatively, fairly successful in representing
the experimental situation, quantitatively, most give order
of magnitude estimates at best [Luthi, 1968; Ikushima,
1970]. There are, however, some very sophisticated
theoretical evaluations [Itoh, 1975] that seem to give good
qualitative and quantitative results.

This page has been removed because of the unavailability of copyright permission.

The page contained a figure showing ultrasonic attenuation peaks characteristic of an antiferromagnetic phase transition. The figure was taken from a paper by Cracknell and Semmens that appeared in the Journal of Physics C, vol. C4, 1971, p1513.

4.2 Measuring Ultrasonic Attenuation

The study of the ultrasonic attenuation in a metal requires introducing a well-defined beam of sound waves of a known frequency into the metal. This is usually accomplished by fixing a piezoelectric material to the end of the specimen. This transducer converts electromagnetic impulses into mechanical waves which then propagate through the specimen. The transducer may also be used for the inverse process of converting a mechanical stress wave into an electrical impulse that can then be recorded.

Quartz is the usual material for transducers. Although other materials are available, e.g. CdS, ZnS, or LiNbO$_3$, quartz is usually preferred as it has a very high Q and therefore has a large response at its fundamental or harmonic frequencies. Quartz is also reasonably easily machined. As the thickness of the quartz transducer determines its fundamental frequency, this machinability along with its high Q allow quartz to be driven over a wide range of frequencies (from about 3 MHz to several hundred megaHertz) when harmonics are included. Cadmium sulfide, on the other hand, is a low Q material and while it can be driven over a continuous range of frequencies, these frequencies are typically about 300 to 800 MHz.

Other advantages of quartz transducers include the relative temperature insensitivity of their mechanical

properties, and their ability to produce either a
longitudinal or a transverse wave (depending upon how they
are cut).

In order to measure the ultrasonic attenuation the
transducer is bonded to the sample and then excited by a
short duration electromagnetic pulse tuned to the
fundamental, or an odd harmonic of the fundamental,
frequency of the transducer. The transducer converts this
electromagnetic pulse into a pulse of mechanical waves, of
the same frequency, which then propagate into the specimen
and are nearly perfectly reflected at the opposite end of a
properly prepared specimen. If the opposite ends of the
specimen are smooth and parallel then the pulse returns
through the specimen to the transducer-sample interface.
Here, a very small part of the signal is sampled by the
transducer, while most of the signal is reflected back into
the sample. The transducer reconverts the vibration into an
electromagnetic pulse, which may then be displayed on an
oscilloscope.

During each trip through the sample, energy is
scattered out of the sound wave by the processes described
above. Therefore each time the sound wave returns to the
transducer-sample interface it carries less energy, and the
oscilloscope displays a series of pulses, or echoes,
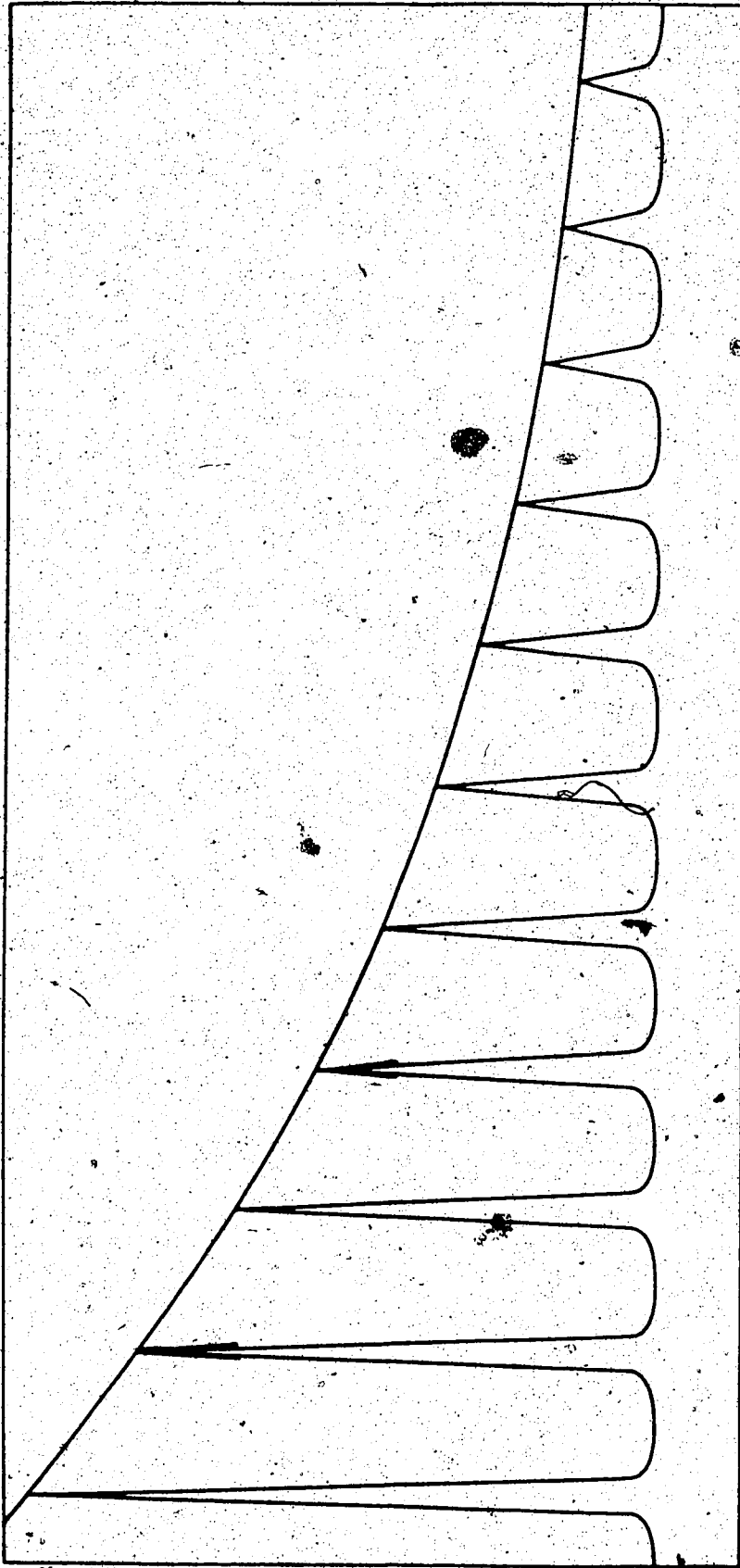diminishing in size with each round trip (see figure 4-5).

figure 4-5 Decaying echo train showing
exponential envelope, and strobed
sections.

28

By fitting an exponential curve to the envelope of this
decay, a value for the ultrasonic attenuation coefficient,
α, can be determined.

This result for the ultrasonic attenuation will be
representative of the actual attenuation in the sample if
certain conditions are met in preparing the sample.

The two most important considerations in the
preparation of a sample for attenuation measurements are the
transducer-bond-sample interface, and whether or not the two
opposite edges that reflect the sound wave are plane
parallel.

The requirement of plane parallel ends is fairly
strict. Any originally parallel wave that is reflected
through a small angle returns to the transducer at an angle
which increases, of course, with each round trip through the
specimen. The incidence of the wave at an angle causes
different areas of the transducer to see different phases of
the wave, which results in degradation of the exponential
envelope. Even a small degree of non-parallelism produces
minima in what should be an exponential envelope [Truell et
al. 1969, p107].

Bonding the transducer to the specimen is also very
important and produces special difficulties. Since all
information about the attenuation in the sample is
transmitted across that interface, it is clearly desirable

to minimize the energy lost at this point. Any energy lost during the exchange of information between the transducer and the sample will directly affect the oscilloscope display and disguise the actual attenuation.

The transducer is usually attached to the sample with a thin layer of grease or cement. Cementing the transducer onto the sample with a thin layer of epoxy usually gives excellent contact, but such a permanent arrangement has certain disadvantages. If the measurement requires cooling to very low temperatures the thermal stresses between the transducer and the sample may be sufficient to break the bond. With a permanent cement bond the transducer is very likely to break as well. With this problem in mind, popular bonding agents are silicone vacuum grease and Nonaq stopcock grease. A thin layer of one of these greases provides good contact between the transducer and the specimen. If the bond should crack when cooled it is unlikely to break the transducer, and the bond is easily remade at room temperature.

Diffraction and sidewall reflection are other sources of beam loss that should be kept in mind.

Diffraction is the spreading out of the beam, with the result that the transducer may see only a small part of the returning beam. Its effects are the largest at very low frequencies, and when the transducer is small compared to the sample diameter.

Sidewall reflections can alter the beam in two ways: the sidewall reflected beam, being out of phase, can interfere with the signal thus degrading the output; and, the contact with the sidewall may result in mode conversion, i.e., part of the energy of a longitudinal wave, for example, may be converted into a transverse vibration which the transducer will not be sensitive to, again resulting in a false source of attenuation.

While great care is taken to minimize the energy losses due to these effects, it is still difficult to ensure that the attenuation computed from the oscilloscope display is the actual attenuation in the sample. Remaking the grease bond, for example, will frequently change the magnitude of the observed attenuation. The bond will not have exactly the same properties, e.g. thickness, as the previous one, even though the bond is made in the same manner.

It is also very difficult to estimate theoretically the magnitude of the losses due to these effects, though some calculations do exist [Truell et al. 1969, p88].

For these reasons it is usually more convenient to monitor the attenuation and observe how it changes as some other property (temperature, magnetic field, etc.) is varied, rather than being too concerned with the true magnitude of the attenuation coefficient in the sample.

In some experiments, though, the nature of the experiment allows for a reasonable determination of the actual attenuation coefficient. When measuring attenuation in superconductors [David, 1964] the attenuation well below the transition is assumed to be due to impurity scattering, and the various sample preparation problems only. This is taken to be the zero level, as the attenuation is theoretically zero in this region With this value subtracted, the attenuation coefficient obtained at higher temperatures can be taken as the actual value in the sample.

In measurements on antiferromagnetic materials, however, such conditions do not exist. There is no convenient zero level, as the attenuation in these materials peaks near the transition temperature. This makes it very difficult to determine the actual absolute value of the attenuation, therefore quantitative comparison to the theory is difficult in these materials. Qualitative analysis is usually possible though, since it is the shape of the peak that is of interest.

5. THE EXPERIMENT

5.1 Sample Preparation

The $CeAl_2$ sample used in these experiments was polycrystalline. It was prepared by melting the stoichiometric amounts of cerium (99.9% pure) and aluminum (99.996% pure) together in an arc furnace under an argon atmosphere. The resulting ingot was then annealed at 900 °C for one week. An x-ray powder pattern analysis showed the cubic-Laves structure expected for $CeAl_2$, with no evidence of secondary phases [Kadowaki, 1986].

A rectangular sample with squared ends, suitable for ultrasonic measurements was then spark cut from the ingot. Although one has an ideal shape in mind: i.e.; sufficient length to allow the electronics time to reset between each returning echo, and dimensions that will support the transducer as well as minimize the sample losses discussed earlier; the resulting dimensions of the sample are, of course, limited by the size and shape of the initial ingot.

After the ingot had been cut into an appropriate shape the ends were made plane-parallel. This was achieved by mounting the sample on a metal plate with silver print, and then spark cutting one end of the sample. The sample was then removed from the mounting plate, leaving the plate fixed in place in the spark cutter. The sample was then turned end for end and the cut end attached to the plate

The freshly exposed end was then cut. The sample was turned end for end again and cut for a third time. Since the mounting plate is not moved during this procedure it maintains precisely the same position relative to the cutting blade. Cutting the ends of the sample in this manner, therefore, makes each end parallel with the mounting plate and, as a result, parallel with each other.

The ends were then carefully polished with #1000 carborundum paper. The parallel orientation of the ends was preserved using a simple piston and cylinder apparatus to keep the carborundum paper parallel to the ends of the sample.

The result of the above procedures was a polycrystalline sample of $CeAl_2$, 7.85 mm long and having an approximately square (about 4 mm on a side) cross-section.

5.2 Data Collection

The ultrasonic attenuation data were collected automatically using a Matec model 6000 Pulse Generator and Receiver (or Main Frame), and its attendant equipment. Specifically: a model 960 R.F. Plug-In; a model 120 Master Synchronizer; and a model 2470 Automatic Attenuation Recorder. When set up as in figure 5-1, the above equipment generates the R.F. signal that drives the transducers; receives and displays the returning echoes; and automatically computes and records the attenuation.
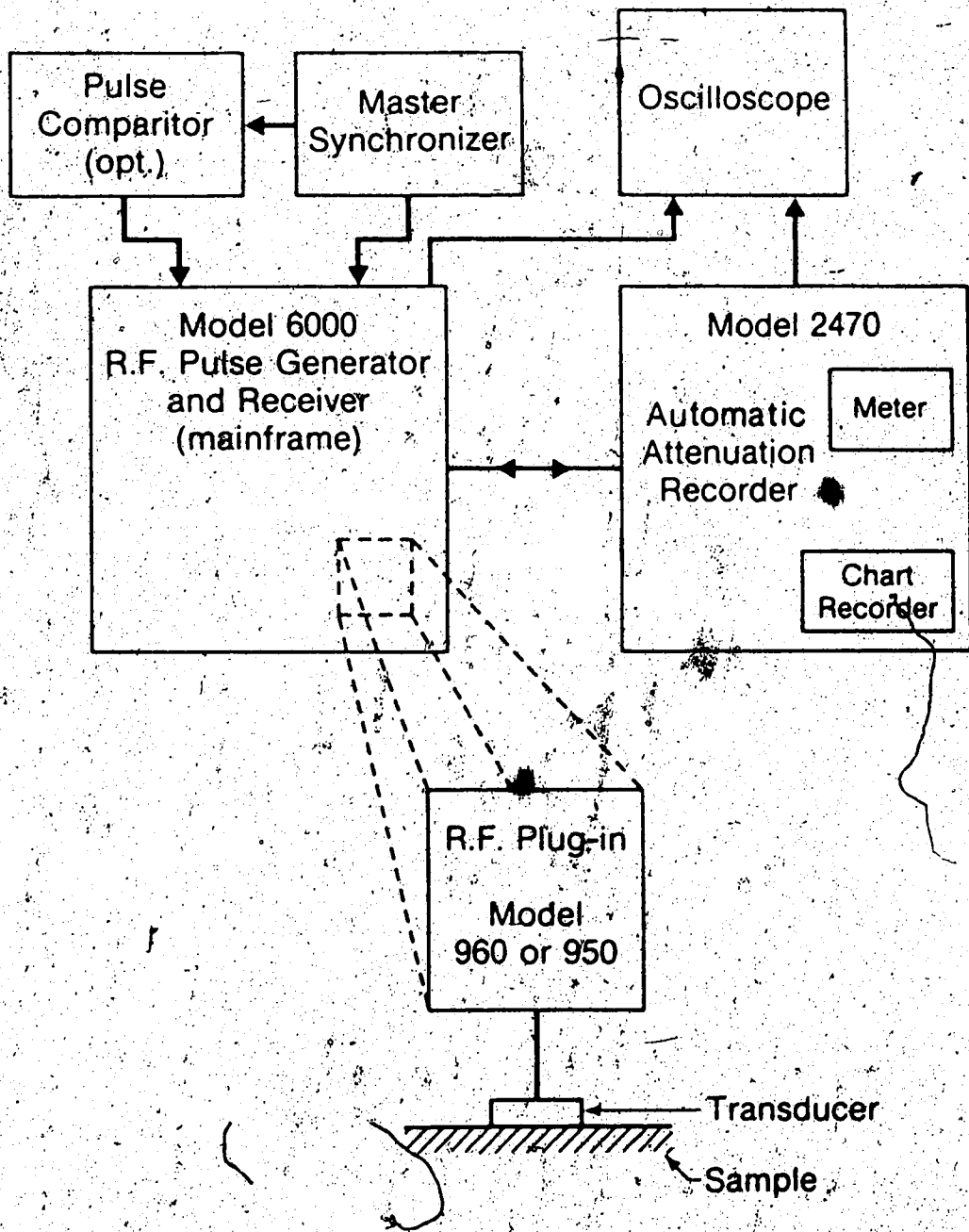
figure 5-1 Schematic diagram of equipment set-up.

The Pulse Generator and Main Frame, with the appropriate
R.F. Plug-In (Model 960 in this case), generate a pulsed
R.F. signal that drives the quartz transducer. This signal
can be tuned to match the fundamental, or an odd harmonic of
the fundamental frequency of the transducer. The returning
echoes in the sample are then picked up and reconverted by
the transducer to an R.F. signal and returned to the
Mainframe. Here the echoes are amplified and detected,
after which they are displayed on an oscilloscope, and
coupled to the Automatic Attenuation Recorder.

The Automatic Attenuation Recorder allows the
operator to select any two echoes in the ultrasonic echo
train and differentially compare their resultant D.C.
voltages using a logarithmic voltmeter. Two delay
generators are triggered by the main driving pulse, these in
turn drive two echo selectors. The echo selectors pass only
a single echo each, rejecting all other echoes as well as
the main driving pulse. Intensification strobes from the
delay generators are applied to the oscilloscope display to
identify the selected echoes (figure 4-5). After
amplification the selected echoes are fed into Peak
Detectors which obtain D.C. voltages that are directly
proportional to the amplitudes of the selected echoes.
These voltages are then fed into a Differential Logarithmic
Amplifier, which computes the attenuation and displays it on
a meter and/or a chart recorder.

Such a setup allows a continuous scan of the ultrasonic attenuation to be made as some other variable (e.g. temperature or applied magnetic field) is changed.

The transducers used in this experiment were gold plated x-cut quartz crystals, which produce a longitudinal or compression wave in the sample. Transducers having fundamental frequencies of 5, 10, and 15 MHz were tried. Although there was some early limited success driving the 5 MHz transducers at 25 MHz, the best echoes at liquid helium temperatures were obtained with the 10 and 15 MHz transducers operating at their fundamental frequencies.

The 5 and 10 MHz transducers were produced by the Valpay Crystal Co. and were 3 mm in diameter. The 15 MHz transducers were cut from a square piece of transducer material with a diamond wheel and then shaped to about 3 mm in diameter to fit the end of the specimen.

The transducer was bonded to the end of the specimen with a very thin layer of silicone vacuum grease. The bond was made by spreading a thin layer of grease on a second piece of (clean) metal. The transducer was then placed onto this grease and then carefully slid off the metal and onto the sample. The grease that clings to the transducer as it is slid over forms the bond. This technique results in a very thin, uniform layer of grease between the sample and the transducer. This layer is adequate to couple the
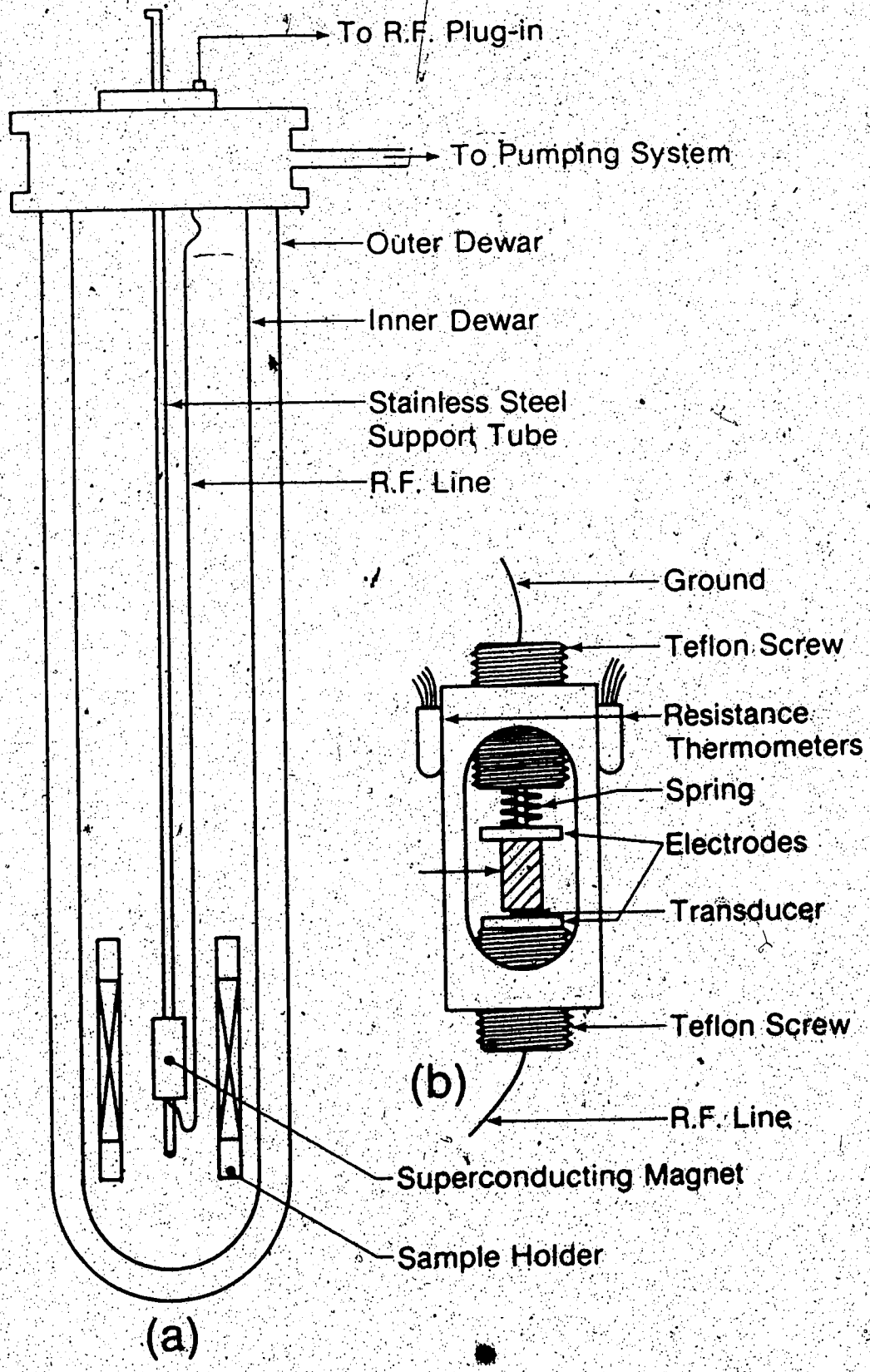
transducer to the sample, but is not so thick as to interfere with the transfer of information between the transducer and the sample.

One transducer was used to initiate the ultrasonic pulse in the sample and to detect the returning echoes. The use of a second transducer as the receiver requires another bond to be made. This, of course, greatly increases the difficulty in getting echoes, as two low attenuation bonds are now required. Chances of bond failure when the system is cooled are increased as well.

The sample was mounted in a sample holder, the top of which was designed to fit a ^{4}He cryostat. The sample holder was of sufficient length to suspend the sample in the centre of a superconducting solenoid mounted in the ^{4}He dewar (figure 5-2a). The sample itself was mounted between two copper electrodes held in place, in a hollow brass block, by two teflon screws (figure 5-2b). One of the electrodes was spring loaded which made it possible to adjust the pressure exerted on the sample and transducer by the electrodes. This pressure was adjusted to optimize the echo train.

The electrode that pressed against the transducer was linked with a shielded wire to the top of the sample holder, from where it was connected with a coaxial cable to the Pulse Generator. The electrode on the opposite end of the sample was connected to ground.

figure 5-2 ^{4}He Cryostat and Sample Holder

To R.F. Plug-in

To Pumping System

Outer Dewar

Inner Dewar

Stainless Steel
Support Tube

R.F. Line

Ground

Teflon Screw

Resistance
Thermometers

Spring

Electrodes

Transducer

Teflon Screw

(b)

R.F. Line

Superconducting Magnet

Sample Holder

(a)

The sample was cooled by immersing it directly into a liquid helium bath in a glass ^{4}He cryostat. Temperatures of about 1.8K were achieved by reducing the pressure over the liquid helium bath with the pumping system shown in figure 5-3.

The pumping rate, and therefore the rate of change of the temperature, was controlled with a manostat (figure 5-4a). By slowly opening valve A, and allowing the pump to reduce the pressure in the reservoir tank, the flexible membrane moves and allows the pump to pump on the liquid helium bath (figure 5-4b). When the valve is closed the pump is only able to reduce the pressure over the bath to that of the reservoir. At this point the membrane snaps shut (figure 5-4c) and the pump can no longer reduce the pressure over the helium bath. As long as valve A remains closed the pressure over the liquid helium bath will be maintained at that present in the reservoir. By careful adjustment of the valves the temperature of the liquid helium bath could be slowly decreased from about 4.2K to about 1.80K.

It is important that the temperature change occurs very slowly. This maintains the sample and the bath in thermal equilibrium (or very close to thermal equilibrium), and ensures that the temperature of the bath is uniform and corresponds correctly to the vapour pressure measured above the bath. Pumping too quickly leads to temperature gradients in the liquid helium and the temperature indicated
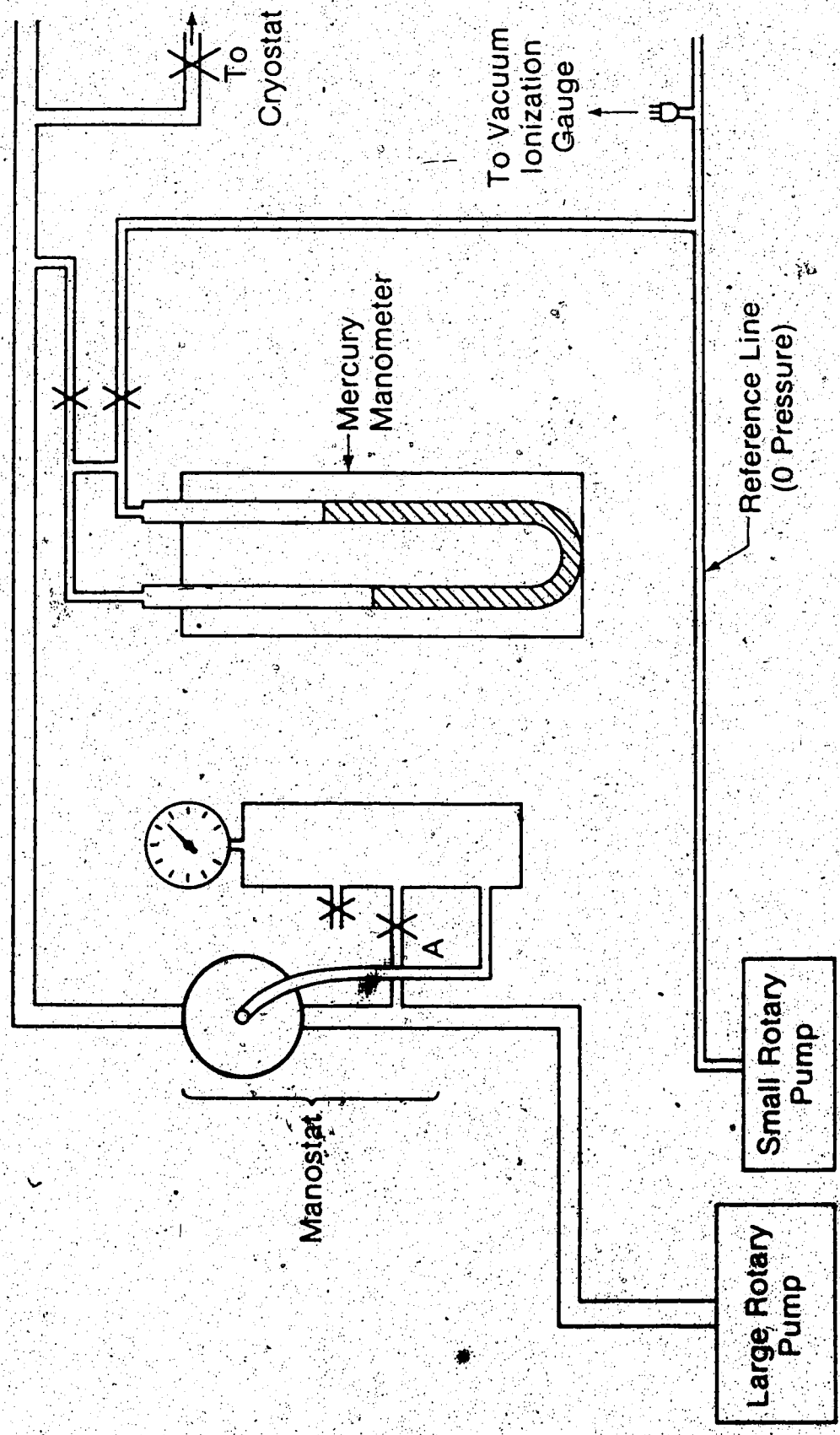
figure 5-3   Pumping system

To Cryostat

To Vacuum
Ionization
Gauge

Mercury
Manometer

Reference Line
(0 Pressure)

Manostat

A

Small Rotary
Pump

Large Rotary
Pump

(a)

To Cryostat

P_0

Membrane

P'
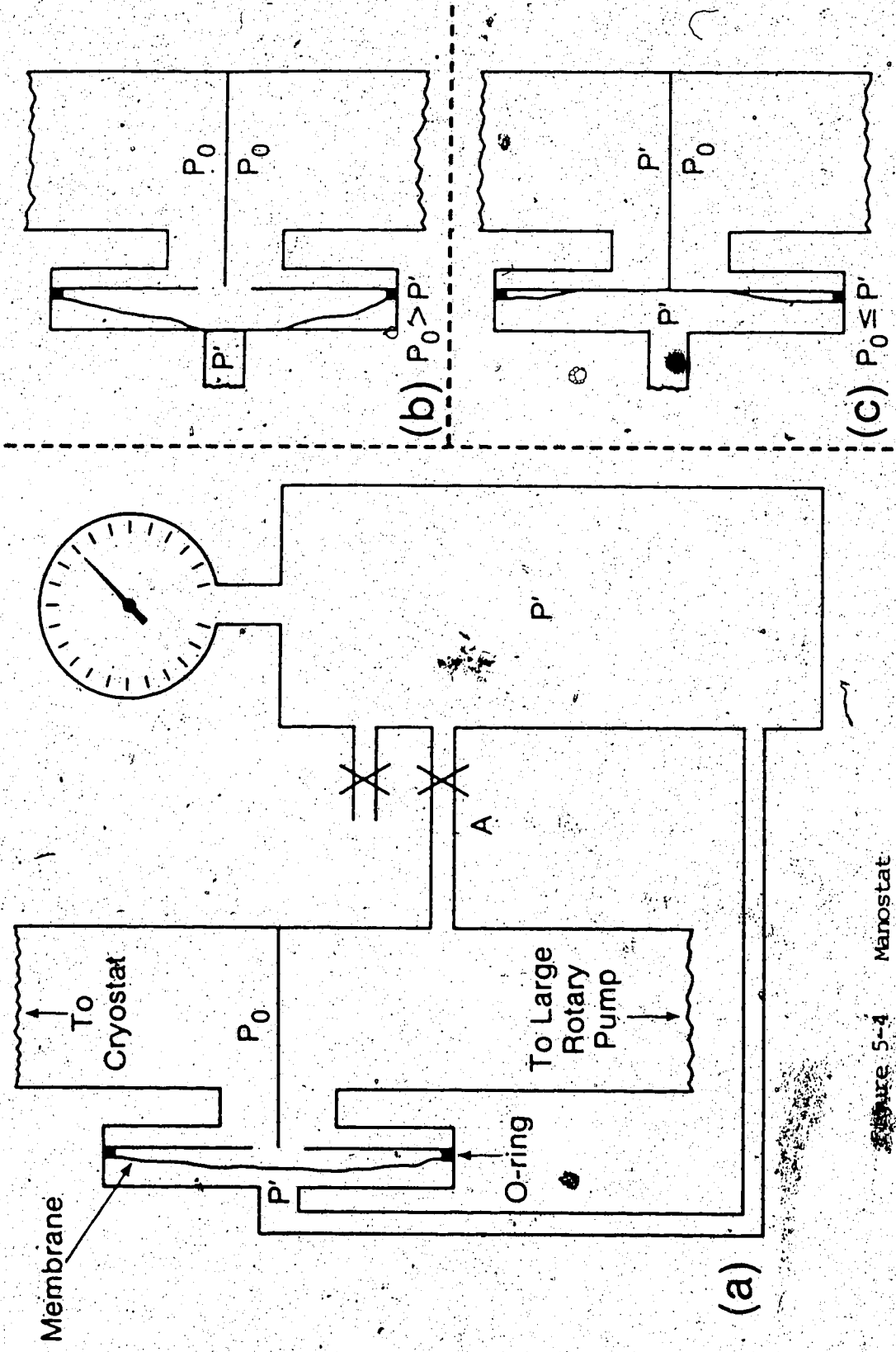
O-ring

To Large Rotary Pump

A

P'

(b) $P_0 > P'$

P_0

P_0

P'

(c) $P_0 \leq P'$

P'

P_0

Figure 5-4   Manostat.

by the vapour pressure will not be the same as the actual
temperature of the sample.

The temperature was determined, in the first few
runs, from the vapour pressure over the liquid helium bath.
The pressure was measured with a mercury manometer and
converted to temperature using a standard set of tables
[Brickwedde et al. 1960].

For convenience and accuracy, two types of
resistance thermometer were employed to determine
temperature in later runs. The installation of these
devices made recording the temperature on the chart recorder
much easier for one person to manage. It was very difficult
for one person to follow the manometer and the attenuation
recorder simultaneously. Also, the position of the pressure
sensor in the pumping line (see figure 5-3) may have
resulted in some question about the accuracy of the pressure
reading.

Two types of thermometer were used. A germanium
resistance thermometer (#904) which had been calibrated with
an accuracy of ±2 mK against helium vapour pressure [Rogers,
1968]. The other sensor was a Carbon Glass resistance
thermometer (CGR-1 500 #C5176) from Lake-Shore Cryotronics
Inc. This sensor was calibrated against the Germanium
thermometer during the experiment. The Carbon-Glass
thermometer was included because of its insensitivity (< 2%)
to magnetic fields.

These thermometers were taped to the brass block of the sample holder (figure 5-2b). Putting the thermometers in direct contact with the sample holder, and very close to the sample ensures that the temperature detected by the sensors is as close as possible to the actual temperature of the sample.

The resistance of each thermometer was measured using a four-terminal Potentiometric Conductance Bridge (PCB Bridge) made by the S.H.E. Corporation. Two such bridge were used so that each thermometer could be monitored simultaneously. The bridges were checked for accuracy against a standard Four Terminal Variable Resistor type 9801-T from Guildline Instruments Ltd.

5.3 Experimental Method

The transducer was bonded to the sample with silicone grease, and the sample was then placed into the sample holder.

The Pulse Generator and Receiver were then tuned, and the gain adjusted to obtain the best possible echoes. The pressure of the electrodes against the sample and transducer was also adjusted if necessary to improve the echoes. If the echoes were of very poor quality, or there were no echoes at all, the bond was remade, and the sample holder reassembled.

When a reasonable echo pattern was obtained at room temperature, the sample was immersed in a bath of liquid nitrogen, and the equipment adjusted to optimize the echoes. If the echoes were of fairly good quality the nitrogen was blown out and the dewar filled to just above the sample with liquid helium. If the echoes were unsatisfactory at liquid nitrogen temperatures, the sample holder was removed from the dewar system, wrapped in a plastic bag to prevent moisture condensation on the sample, and warmed back up to room temperature. At room temperature the bond was remade and the above procedure repeated.

During the course of the experiment it was found that if the echoes were of even marginal quality at 77K, there was a reasonably good chance that they would improve

when cooled to liquid helium temperatures. If the echoes were not good enough, or the bond broke and the echoes were lost altogether then, of course, the sample had to be warmed back up to room temperature. The liquid helium was boiled off and the above procedures repeated.

When the echoes were strong enough to allow attenuation measurements to be made the helium dewar was filled the rest of the way. This provided enough helium to make two or three scans from about 4.2K to about 1.8K over the space of several hours.

After the helium had been transferred, the vacuum system was set up to pump on the helium bath and the chart recorder on the Automatic Attenuation Recorder turned on.

As the temperature was slowly decreased the chart recorder made a continuous record of the attenuation in the sample. The attenuation in the sample was matched to the corresponding temperature in the sample by reading either the vapour pressure from the mercury manometer, on runs #1-3, or the value displayed by the conductance bridge, on later runs, and marking this reading directly on the chart recording. After the experiment was finished, these vapour pressure, or conductance, values could be converted to temperatures, and a graph of attenuation as a function of temperature could be drawn.

For the most accurate determination of the

temperature at the sample the ultrasonic attenuation was
recorded only when scanning downwards in temperature. The
bath was then warmed back up to about 4K and the temperature
allowed to stabilize before the next run commenced. This
procedure is necessitated by the thermal gradients present
in the liquid helium as the bath warms up. The vapour
pressure over the helium will no longer be related to the
temperature of the helium bath, especially if the bath is
warmed by circulating exchange gas.

6. RESULTS

With the equipment and procedures described in the previous sections, measurable echoes were obtained at liquid helium temperatures on three separate occasions. The first two runs were made with a 10 MHz transducer, while a 15 MHz transducer was employed in later runs. The change of transducers was necessitated when the 10 MHz transducer was broken during the preparation for a run. Three squares were then cut from a rectangular piece of 15 MHz transducer material, and shaped into disks 3mm in diameter. These transducers were used in the later runs, which were made several weeks after the initial runs at 10 MHz.

While the ultrasonic attenuation was being measured, the carbon-glass thermometer was calibrated against the germanium thermometer. During this calibration the vapour pressure above the liquid helium bath was also noted. This was done in order to compare the temperature, as indicated by the vapour pressure, to the temperature given by the calibrated germanium thermometer. It was found that the germanium thermometer agreed with the vapour pressure to within about 30 mK (or less than 1%), when the temperature was changing slowly. When the temperature changed more rapidly (above 4K) the two results differed by no more than 4%.

The ultrasonic attenuation results at 10 MHz are shown in figure 6-1. The temperature range between 2 and 4K

figure 6-1 Ultrasonic attenuation in CeAl$_2$ as a function of temperature (10 MHz).
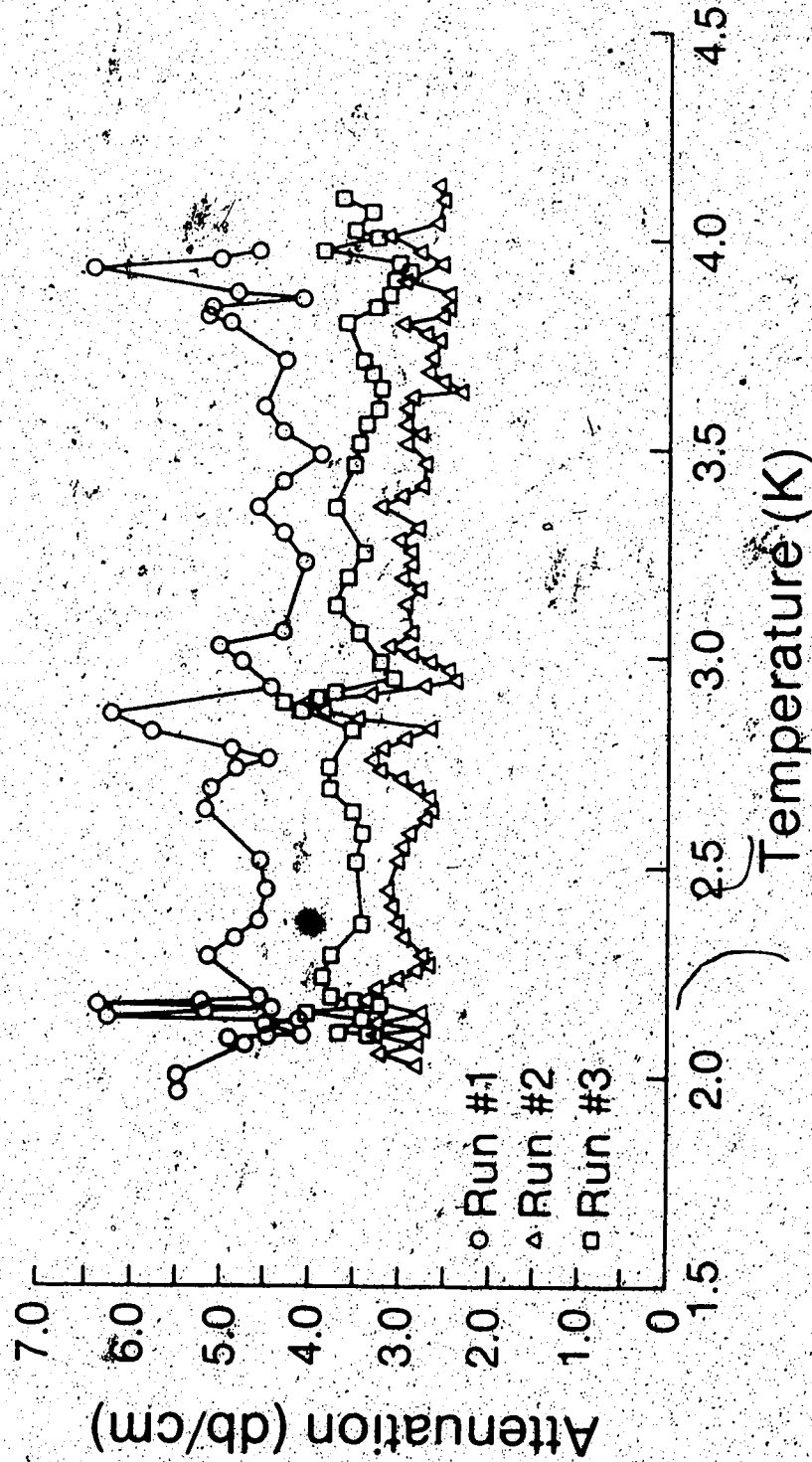
was scanned three times; with the sample warmed to room temperature and the bond remade after the first run. In both cases the echo train consisted of three fairly strong echoes. The echoes were separated in time by about 3.0 microseconds, which gives a value of $(5.2 \pm 0.7) \times 10^5$ cm/s for the velocity of the sound waves in the specimen.

The first thing one notices about the curves in figure 6-1 is the amount of fluctuation present in the attenuation. At first glance, there does not appear to be much of interest going on. Closer inspection of the curves, however, shows three features of interest.

Two peaks can be seen to rise up well above the other fluctuations in run #1. One peak is at about 3.9K and the other is at about 2.85K. There is also a a very rapid fluctuation, of large magnitude, in the attenuation at about 2.17K.

Two of these features: the rapid fluctuations below 2.17K, and the broad attenuation peak at 2.85K; also appear in runs #2 and #3. These two runs were made three days later after the sample had been warmed to room temperature and the bond remade. Although the large peak at about 3.9K is not really evident in the other two runs, there is a certain amount of fluctuation in the attenuation in this region in these runs.

The peak at 3.9K would seem to correspond to the

antiferromagnetic transition that is known to occur at about this temperature in $CeAl_2$. If this is the case, it is odd that the transition does not show up more strongly in the other two runs, especially since the peak at 2.9K is present in all three runs.

The extreme variation of the attenuation, beginning just above 2K, that occurs in all three runs can be associated with the λ-point of liquid helium. The helium bath separates into helium I and the superfluid helium II at this temperature. Since the $CeAl_2$ sample is in direct contact with the liquid helium it is not surprising that the attenuation in the sample could be influenced by the agitation in the bath during the transition. Having been alerted by the results of the first run, a close watch was kept on the helium bath in runs two and three. The helium was observed to be in a very agitated state (i.e. in transition) when these rapid fluctuations in the attenuation were occurring.

It is also possible that the superfluid HeII could penetrate (via microcracks) the sample itself. This possibility is indicated by the continuation of the attenuation to fluctuate below the λ-point transition.

The broad peak in the attenuation at 2.9K is very prominent in runs #1 and #2, and only slightly less so in the third run. Since the peak appears in all three runs,

that is, it reappears even after the sample had been warmed to room temperature, it would seem that there is a phase transition of some sort in the sample at that temperature.

There are, however, several points to consider about this possibility.

First of all there are no corresponding anomalies reported, at this temperature, in the other transport properties. Resistivity, thermal conductivity [Bauer et al. 1982], susceptibility [Barbara et al. 1977], and specific heat [Armbruster & Steglich 1978] are all smooth in this region, although they show the transition at 3.9K.

Another consideration is the shape of the peaks themselves. The three peaks at 2.9K are all rather broad, and do not resemble the shape expected (figure 4-4) for a magnetic transition. They do not have the very sharp peak, and the negative curvature indicative of the logarithmic dependence expected from equation 4-11.

With these results in mind, the 15 MHz transducers were prepared to continue the investigation of this region.

During the attempts to produce workable echoes at low temperatures with the new transducers, it was observed that the cracking on the surface of the sample was becoming more extensive. Cracks had begun to appear on the polished ends of the sample. Although there had been some tiny
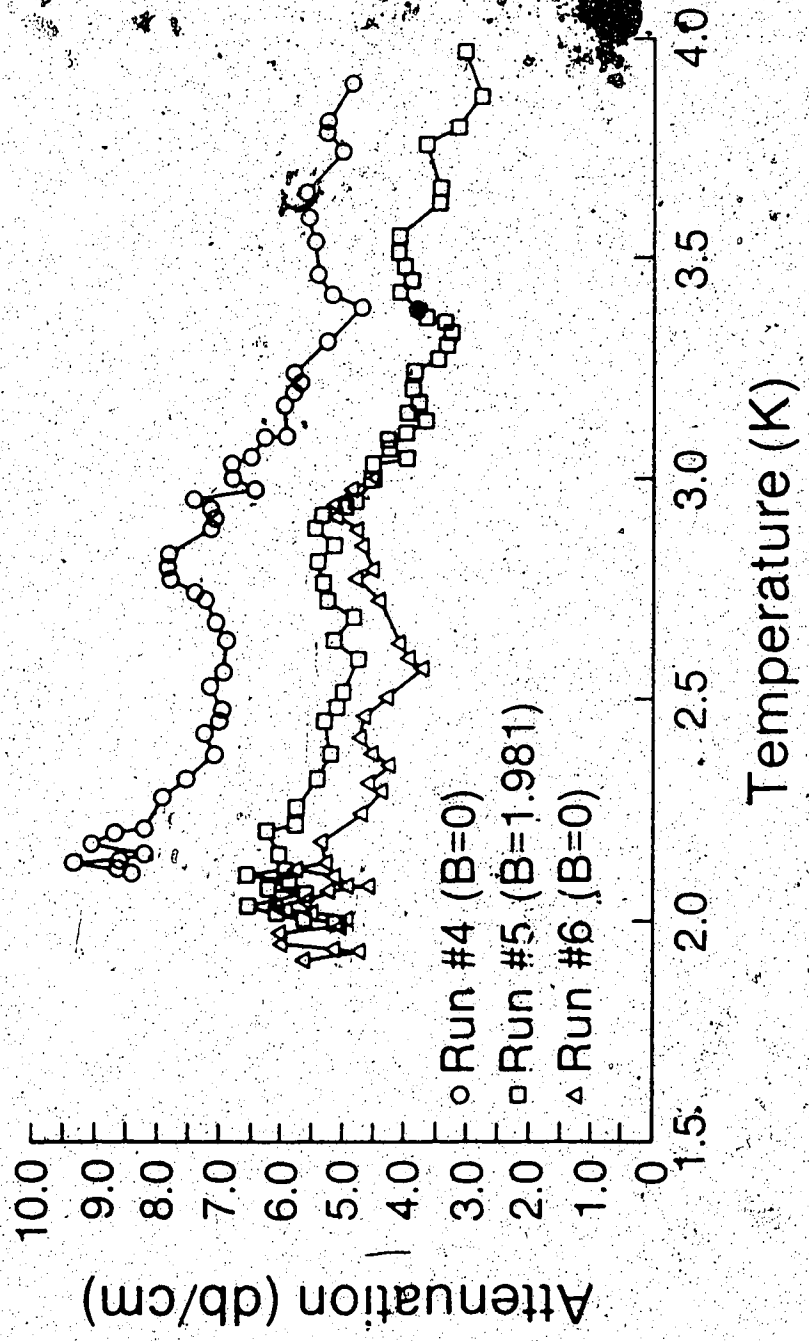
cracks on the sides of the sample when the runs at 10 MHz were made, the ends of the sample were unblemished, at that time.

It was also much more difficult to get measurable echoes in the sample. The attenuation was large enough that when one good echo was found at liquid helium temperatures, it was decided to sit on it and measure the attenuation with the 'single echo' option on the Attenuation Recorder. The height of the echo peak is compared with a constant internal voltage to find the attenuation. Only changes in attenuation can be measured with this technique.

The attenuation curves resulting from three scans of the 2-4K temperature range, at 15 MHz, are shown in figure 6-2. All three curves have the same general shape, showing an overall increase in attenuation as the temperature is decreased. The structure evident in the first three runs, however, is clearly absent. The only feature these curves have in common with those in figure 6-1 is the rapid fluctuation of the attenuation below the λ-point. The attenuation peaks at 2.9K and 3.9K are no longer seen.

The second run (#5 in figure 6-2), of this set, made in a 1.98T applied magnetic field, has a lower attenuation than the first run (#4) made in zero field. However, since the curves for runs #4 and #5 seem to be essentially parallel, and the attenuation of run #6 (where the applied field is again equal to zero), is about the same as the run

figure 6-2 Ultrasonic attenuation in CeAl$_2$ as a function of temperature (15 MHz).

o Run #4 (B=0)
□ Run #5 (B=1.981)
△ Run #6 (B=0)

Attenuation (db/cm)

10.0
9.0
8.0
7.0
6.0
5.0
4.0
3.0
2.0
1.0
0

1.5   2.0   2.5   3.0   3.5   4.0

Temperature (K)

in the applied field, there does not appear to be anything special in this difference.

In order to suggest a possible explanation for these results we consider two factors: the gradual deterioration and cracking of the sample, and the incommensurate magnetic ordering of $CeAl_2$.

This incommensurate ordering of the magnetic moments could lead to an internal strain on the crystal. The anisotropy of the internal magnetic fields is known to be quite large [Barbara et al. 1977]. Such an internal strain could gradually build up in the sample as the temperature is slowly decreased. The peak in the attenuation at 2.9K could then be an indication of the point where the internal strain had built up to such a level that the crystals either fractured or shifted to relieve the strain.

We note that the anomalous attenuation peak in figure 6-1 occurs at essentially the same temperature in all three runs. It is shifted only slightly higher in temperature (from 2.85K to 2.9K) between runs #1 and #2.

If the release of the strain does not catastrophically change the microstructure of the sample, is possible that the temperature at which the strain is released would not change too much over consecutive runs. Frequent cooling and warming of the sample, however, would continue to weaken the sample, increasing the microcracking

and cracking to the point where the degradation of the
sample would be sufficient to disguise any structure in the
ultrasonic attenuation.

The overall degradation of the sample noted above is
probably contributed to by other factors in addition to the
strain induced by the magnetic ordering. Thermal expansion
[Croft et al. 1978A] and the large anisotropic
magnetostriction [Croft et al. 1978; Zieglowski et al. 1987]
can be expected to contribute to the degradation of the
crystal during cycling between helium temperatures and room
temperature. Other experimentalists have experienced
similar degradation problems when measuring the transport
properties of $CeAl_2$ down to liquid helium temperatures
[Onuki, 1986]. It is very difficult to get a continuous
measurement of, say, resistivity over the range 4-300K
without small discontinuities caused by the crystal cracking
under strain.

There is no indication in any of the curves of a
second phase transition near the Neel point. This is not to
say, however, that such a transition does not exist. It may
be that in zero field the transition is too close to the
Neel peak to be distinguished. When the runs were made in a
high magnetic field, which should have separated the two
transitions (if indeed the second one exists), the sample
had deteriorated to such an extent that even the Neel point

was no longer visible.   Any secondary peak would also be

lost.

7. CONCLUSION

The ultrasonic attenuation in a polycrystalline sample of the dense Kondo material, $CeAl_2$, was measured. It proved very difficult to achieve measurable echoes at liquid helium temperatures.

These measurements have shown an anomalous peak in the ultrasonic attenuation at 2.9K. However, before detailed measurements on its behaviour in a magnetic field could be made, the condition of the sample had deteriorated to the point where even the Neel point could not be seen. This sample deterioration also prevented any detailed investigation of the magnetic phase diagram. There was no evidence, however, in zero field, of a second transition near the Neel point.

The shape of the peak at 2.9K along with the evidence of the other transport properties seemed to rule out a magnetic transition at this point. It was suggested that the incommensurate nature of the magnetic ordering could cause an internal strain on the sample. The peak at 2.9K could then indicate the point where the crystals in the sample shifted or cracked to relieve the strain.

It is also possible, of course, that the peak at 2.9K was due to some other effect; something more inherent to the properties of the compound. A structural change, or some unsuspected phase transition for example.

Since the degradation of the present sample is sufficient to disguise any structure in the ultrasonic attenuation (figure 6-2), new samples of $CeAl_2$ would have to be prepared to test such a possibility.

It may also be desirable to avoid putting the sample in direct contact with the liquid helium bath to limit the stresses involved in cooling the sample. This would involve encasing the sample in some kind of sealed holder, and the temperature could be decreased slowly. This would, however, greatly increase the difficulty of the experiment as there would be one more step to go through should the bond fail, and it would take longer to find out whether this would happen.

Such an effort would be worthwhile as ultrasonic attenuation measurements in several new samples should settle the nature of the peak at 2.9K. If the anomalous peak is indeed caused by internal strain building up below the Neel point, the position of the peak should be dependant on the internal microstructure of the sample. With different microstructure in different samples one would expect the position of the peak to change form sample to sample, or perhaps be absent altogether. If the peak is less transient and occurs at 2.9K in all samples, some other explanation may be necessary.

REFERENCES

1. Aarts J., F.R. de Boer, P.F. Chatel, 1985, J. Magn. Magn. Mater., 49, 271.

2. Armbruster H., F. Steglich, 1978, Solid State Communications, 27, 873.

3. Ashcroft N.W., N.D. Mermin, 1976, Solid State Physics, (Holt, Rinehart, and Winston)

4. Barbara B., J.X. Boucherle, J.L. Buevoz, M.F. Rossignol, J. Schweizer, 1977, Solid State Communications, 24, 481.

5. Bauer E., E. Gratz, W. Mikovits, H. Sassik, H. Kirchmayr, 1982, J. Magn. Magn. Mater., 29, 192.

6. Beyer R.T., S.V. Letcher, 1969, Physical Ultrasonics, (Academic Press, New York)

7. Bhatia A.B., 1967, Ultrasonic Absorption, (Oxford University Press)

8. Bredl C.D., F. Steglich, K.D. Schotte, 1978, Z. Physik, B29, 327.

9. Brickwedde F.G., H. van Dijk, M. Durieux, J.R. Clement, J.K. Logan, 1960, Journal of Research of the National Bureau of Standards-A. Physics and Chemistry, 64A.

10. Buschow K.H.J., H.J. van Daal, 1969, Phys. Rev. Lett. 23, 408.

11. Cornut B., B. Coqblin, 1972, Phys. Rev. B5, 4541.

12. Cracknell M.F., A.G. Semmens, 1971, J. Phys. C4, 1513.

13. Croft M., I. Zoric, R.D. Parks, 1978, Phys. Rev. B18, 345.

14. Croft M.C., I. Zoric, R.D. Parks, 1978A, Phys. Rev. B18, 5065.

15. Croft M.C., H.H. Levine, 1980, Phys. Rev. B22, 4366.

16. David R., 1964, Philips Research Reports 19, 524.

17. Doniach S., 1977, Physica 91B, 231.

18. Franck J.P., F.D. Manchester, D.L. Martin, 1961, Proc. Royal Soc. A263, 494.

19. Hill R.W., J.M. da Silva, 1969, Phys. Lett. 30A, 13.

20. Ikushima A., 1970, J. Phys. Chem. Solids 31, 283.

21. Itoh Y., 1975, J. Phys. Soc. Japan 38, 336.

22. Kadowaki K., 1985, Private Communication.

23. Kadowaki K., 1986, Private Communication.

24. Kondo J., 1964, Prog. Theor. Phys. 32, 37.

25. Luthi B., R.J. Pollina, 1968, Phys. Rev. 167, 488.

26. Luthi B., T.J. Moran, R.J. Pollina, 1970, J. Phys. Chem. Solids 31, 1741.

27. Mason W.P., 1958, Physical Acoustics and the Properties of Solids, (D. van Nostrand and Company Inc., Toronto)

28. Meissner W., B. Voigt, 1930, Ann. Phys. 7, 761,892.

29. Morse R.W., 1959, Prog. Cryog. 1, 221.

30. Ohkawa F.J., 1983, J. Phys. Soc. Japan 52, 3886.

31. Onuki Y., Y. Furukawa, T. Komatsubara, 1984, J. Phys. Soc. Japan 53, 2734.

32. Onuki Y., 1986, Private Communication.

33. Patthey F., W.-D. Schneider, Y. Baer, B. Delley, 1987, Phys. Rev. B35, 5903.

34. Pippard A.B., 1955, Phil. Mag. 46, 1104.

35. Rogers J.S., 1968, Calibration Report.

36. Rossat-Mignod J., P. Burlet, T. Kasuya, S. Kunii, T. Komatsubara, 1981, Solid State Communications 39, 471.

37. Schefzyk R., W. Lieke, F. Steglich, 1985, Solid State Communications 54, 525.

38. Stewart G.R., 1984, Rev. Mod. Phys. 56, 755.

39. Truell R., C. Elbaum, B.B. Chick, 1969, Ultrasonic Methods in Solid State Physics, (Academic Press, New York)

40. Walker E., H.-G. Purwins, M. Landolt, F. Hulliger, 1973, Journal of the Less Common Metals 33, 203.

41. Wielinga R.F., 1970, Progress in Low Temperature Physics 6, 333.

42. Yoshimori A., H. Kasai, 1984, J. Magn. Magn. Mater. 31-34, 475.

43. Zieglowski J., D. Wohlleben, H.J. Schmidt, E. Muller-Hartmann, K. Winzer, 1987, Phys. Rev. B35, 8595.

VITA

NAME: William Albert Miner

PLACE OF BIRTH: Mayerthorpe, Alberta, Canada

YEAR OF BIRTH: 07/07/1961

POST-SECONDARY EDUCATION: Camrose Lutheran College

The University of Alberta

B.Sc. (1980-1984)

The University of Alberta

M.Sc. (1984-1987)

PUBLICATIONS: 1. K. Kadowaki, A. Umezawa, W.A. Miner

and S.B. Woods, 1987, J. Less

Common Metals, 127, 281

2. J. Jung, J.P. Franck, W.A. Miner

and M. A-K. Mohamed, Phys Rev B (in

press).